FACULTY OF MATHEMATICS AND PHYSICS
Charles University

Summary of doctoral thesis

Jana Doubravová

Automatic and semi-automatic processing of seismograms from local networks WEBNET and REYKJANET

Department of Geophysics

Supervisor of the doctoral thesis: Ing. Josef Horálek, CSc.
Study programme: Physics
Study branch: Physics of the Earth and Planets

Prague 2020

FACULTY
OF MATHEMATICS
AND PHYSICS
Charles University

Autoreferát dizertační práce

Jana Doubravová

Automatické a poloautomatické zpracování seismogramů z lokálních sítí WEBNET a REYKJANET

Katedra geofyziky

Vedoucí dizertační práce: Ing. Josef Horálek, CSc.
Studijní program: Fyzika
Studijní obor branch: Fyzika Země a planet

Praha 2020

Dizertace byla vypracována na základě výsledků získaných v letech 2011-2020 během doktorandského studia na Katedře geofyziky MFF UK a v Geofyzikálním ústavu AV ČR.

Dizertantka:
Ing. Jana Doubravová
Geofyzikální ústav AV ČR, v.v.i.
Boční II/1401, 141 31 Praha 4

Školitel:
Ing. Josef Horálek, Csc.
Geofyzikální ústav AV ČR, v.v.i.
Boční II/1401, 141 31 Praha 4

Oponenti:
RNDr. Jiří Málek, Ph.D.
Ústav struktury a mechaniky hornin AV ČR, v.v.i.
V Holešovičkách 41, 182 09 Praha 8

Dr. Simone Cesca
Helmholtz-Zentrum Potsdam
Deutsches GeoForschungsZentrum GFZ
Telegrafenberg, 14473 Potsdam

Předsedkyně oborové rady:
doc. RNDr. Hana Čížková, Ph.D.
Katedra Geofyziky MFF UK
V Holešovičkách 2, 180 00 Praha 8

Obhajoba dizertace se koná dne 8.9.2020 v 10:00 hodin před komisí pro obhajoby dizertačních prací v oboru Fyzika Země a planet v budově MFF UK, Ke Karlovu 3, Praha 2 v místnosti M252.

S dizertací je možno se seznámit na oddělení postgraduálního studia MFF UK, Ke Karlovu 3, Praha 2, a na webové stránce `www.ig.cas.cz/obhajene-prace`.

Contents

1 Introduction

Automatic processing of seismic data is nowadays a crucial point in seismology. The number of stations operated in global, regional and local seismic networks or deployed in various temporal field experiments has been growing and the stations are mostly running with continuous digital recording. In the last thirty years, observational seismology has undergone a radical progress from autonomous stations equipped with frequency narrow-band seismographs to the networked digital broadband stations with constant Internet access. The seismic processing developed from fairly limited manual procedures (visual event detection and manual readings of travel times and selected amplitudes of detected events) allowed by the analog seismograms on a photographic paper, into near-real time automatic or semi-automatic data processing enabled by the digital seismic data streamed on-line. In the era of the analog recordings only seismograms of prominent events could be analyzed in more details, quantitative processing of seismograms was practically impossible; accordingly there were only sporadic demands on more advanced databases. Digital seismic observations, which started to be increasingly used at the turn of 80's and 90's of the twentieth century, meant a significant milestone in seismology. The main progress was the possibility of quantitative analyses of event waveforms or complete seismograms using advanced processing methods. This together with a progress in data acquisition systems and data transmission technologies led to a development and growth of seismic networks. Especially, continuously recording dense seismic networks produce a huge amount of data. The WEBNET and REYKJANET networks operated in West Bohemia earthquake-swarm region and in South-West Iceland (Chapter 3) are a typical example of that. Data from seismic networks should be quickly accessible and processed as quickly as possible, particularly in case of prominent seismic events or increased earthquake activity. However, it cannot be achieved without up-to-date data transfer, advanced databases, and high level of automated/semi-automated data processing.

First of all, there has been a need to reduce the amount of recorded data so that only target seismic events (e.g. local earthquakes) would be processed. In the initial stage of digital seismic observations the seismic stations were operated in a trigger mode. That means event detection was carried out in real time. Only triggered events were recorded and remaining information was irretrievably lost. The triggering algorithms all relied on some version of STA/LTA (Short-Time-Average over Long-Time-Average). However, the STA/LTA triggering algorithms required precise tuning of the parameters to obtain optimal detection performance for a given task and local conditions. In order to achieve good sensitivity of the triggered recording there has been large number of false records due to disturbances, that had to be excluded from further processing (usually manually); on the other hand some weaker events immediately following stronger ones were undetected due to the raised LTA.

Availability of the high capacity memory storage and computational performance of the relatively cheap computers enabled to meet the growing demands of seismologists for continuous seismograms. Consequently, the recording turned to continual regime which made significant progress in observational seismology allowing to record and preserve whole seismograms including very weak events, long-period waves and seismic noise. However, the changeover to continual recordings resulted in an urgent need for automatic pre-processing of continual records. First of all, a reliable automatic event detection was necessary.

Although automatic processing of records enables near-real time computation of all basic parameters of an earthquake the manual processing is still considered as a true reference. The automatic algorithms often fail in case of multiple and overlapping events, or any case of complicated waveforms. In case of earthquake swarms, the prevailing type of seismic activity in our target areas of West Bohemia/Vogtland and South-West Iceland, the overlapping events are very common. Therefore the automatically processed data are continuously under supervision of an expert. The supervision is usually achieved by some interactive software with Graphical User Interface.

My doctoral thesis concerns automated processing of data from local seismic networks WEBNET and REYKJANET which have been operated in earthquake-swarm areas of West Bohemia and South-West Iceland by the Institute of Geophysics (IG) and Institute of Rock Structure and Mechanics (IRSM) of CAS. I have mainly focused on the development of a reliable detection method of local earthquakes using machine learning based on artificial neural networks (ANN). I trained the ANN for the West Bohemia/Vogtland swarm-like events and put the ANN detector into practice for processing of continual recordings from the WEBNET and REYKJANET networks. Furthermore, I have developed the Seismon_WB program package for seismic data processing of the WEBNET and REYKJANET networks. The software enables manual work together with automatic routines and their interconnection and combination supplemented by a communication with the database as an integral part of the program. Seismon_WB is used as a primary tool for visual interactive processing of continual seismograms and displaying the results. Its concept arose from the necessity to replace an obsolete program Seisbase (Fischer and Hampl [1997]) formerly used for processing the WEBNET data, which enabled to work with triggered recordings only. Both these topics solved in my doctoral thesis are not only of crucial importance for automatic or semi-automatic data processing from networks in question but they are also applicable to other local seismic networks.

2 West Bohemia/Vogtland and Reykjanes Peninsula seismicity

Although earthquakes and also earthquake swarms were intensively studied over many decades the possibilities of recording, processing and interpreting the data are increasing rapidly with the well-known increase of computational power obeying the Moor's law. This together with growing data storage capacity has lead to great progress in observation seismology in recent years, which is more and more focused on detailed investigations of the earthquake-source processes and the Earth's crust/lithosphere structure using broadband recordings from dense seismic networks. Original continuous recordings are stored on special data archive servers preserving all data including ambient seismic noise and unnecessary disturbing or noise signals to be available for re-processing and re-interpretation, when needed. The demand for thorough processing of huge amount of data from local seismic networks WEBNET and REYKJANET results from our ambition to explain the primary causes leading to earthquake swarms in areas with completely different tectonic setting as West Bohemia/Vogtland and the Reykjanes Peninsula in South-West Iceland.

The West Bohemia/Vogtland seismogenic region is situated in the western part of the Bohemian Massif, geographically in the border area between Czechia and Saxony (Vogtland is a southern part of Saxony). It is a unique European intra-continental area affected by Quaternary volcanism that exhibits simultaneous activity of various geodynamic processes. Seismic activity is manifested by repeated occurrence of earthquake swarms, but the mainshock-aftershock sequences may rarely occur. Persistent swarm-like seismicity clusters in a number of small epicentral zones that are scattered in the area of about 40x60 km (see grey dots in Fig.2a). Larger swarms ($\sim M_L > 2.5$) cluster predominantly in the focal zone Nový Kostel which dominates the recent seismicity of the whole region. The swarms usually consist of several thousands of weak earthquakes and their duration is from several days to few months. The depths of foci in the whole area range from 5 to 20 km (e.g. Horálek and Fischer [2010]) but depths between 7 and 12 km are typical of earthquake swarms and mainshock-aftershock sequences (Čermáková and Horálek [2015], Jakoubková et al. [2018]). The region is well known by its fluid activity that is probably closely connected with the local swarm-like seismicity (e.g. Horálek and Fischer [2008], Fischer et al. [2017]). For summarizing information about the area in question refer to Fischer et al. [2014].

Reykjanes Peninsula is the onshore continuation of the mid-Atlantic Ridge that separates two major lithospheric plates, the Eurasian Plate to the east and the North American Plate to the west. The plate boundary on the Reykjanes Peninsula is formed by pronounced en-echelon stepping rift segments and extends from the southwest to the east and forms a pronounced oblique rift along the whole peninsula in length of about 65 km (Sæmundsson and Einarsson [2014]). The plate motion rate on the Reykjanes Peninsula is about 20 mm/yr in E–W direction and about 5 mm/yr perpendicular to it (Geirsson et al. [2010]). The Reykjanes Peninsula is a highly complex geophysical structure with the interaction between volcanic and tectonic activity (Sæmundsson and Einarsson [2014]), most of the Reykjanes Peninsula surface is covered by lava. The Reykjanes Peninsula is one of the most seismically active parts of Iceland, especially at the micro-earthquake level. Swarm-like sequences and solitary events scattered along the plate boundary, both with magnitudes mostly of $M_L < 3$, represent a major part of seismicity on the peninsula. Prevailing depths of the foci on the Reykjanes Peninsula are between 2 and 5 km which is much shallower compared to the focal depths in West Bohemia/Vogtland.

Both West Bohemia and Reykjanes Peninsula earthquake swarms usually contain from thousands to tens of thousands events ($M_L > 0$) which are necessary to be processed to get insight into triggering mechanisms and driving forces of earthquake swarms. Manual processing of continual seismograms from the WEBNET (24 stations) and REYKJANET (15 stations) networks is extremely time-consuming, and therefore it is possible to process manually only stronger events. Consequently many weaker events being recorded with a sufficient signal-to-noise ratio remain untouched. The automatic processing is the only way to achieve as low completeness magnitude as possible which is essential for deeper insight into nature of earthquake swarms.

3 Local seismic networks WEBNET and REYKJANET

Continuous data produced by local seismic network WEBNET and later on also REYKJANET were the main motivation for whole this thesis. WEBNET local seismic network deployed in West Bohemia earthquake-swarm region (latitude $\approx 49.8°$ N to $50.7°$ N, longitude $\approx 12°$ E to $13°$ E) has a history of 30 years of monitoring microseismicity, while REYKJANET operated on the Reykjanes Peninsula (SW Iceland, latitude $\approx 63.8°$ N to $64.1°$ N, longitude $\approx 21.5°$ W to $22.3°$ W) dates back to 2013 only. Both networks are nowadays similar in many aspects. They have the same instrumental equipment, sampling frequency or spatial extent. The difference is that all the WEBNET stations are operating with full data streaming through the Internet, while the REYKJANET stations are still off-line. The WEBNET network has generally lower noise than REYKJANET due to installation in deep vaults and compact bedrock (compare the waveforms in Fig. 1). The stations of REYKJANET are sited on the basement mainly formed by lava fields which is typical for the Reykjanes Peninsula.

Seismicity in the West Bohemia/Vogtland region has been monitored by the WEBNET network since 1991 (Institute of Geophysics [1991], Horálek et al. [2000], Fischer et al. [2010]) and the present configuration of 24 broadband stations covers an area of about 40x25 km (Fig. 2a). The network layout ensures proper areal and azimuthal coverage of the focal area, particularly with respect to the main focal zone Nový Kostel.

The REYKJANET stations were deployed on the Reykjanes peninsula in 2013 (Horálek [2013]) by the Institute of Geophysics and the Institute of Rock Structure and Mechanisms of the Czech Academy of Sciences. The network consists of 15 broadband stations covering an area of 40x25 km similarly to WEBNET (Fig.2b). All the stations so far operated in off-line regime in continuous mode are planned to be upgraded to data streaming via Internet.

At present, the WEBNET and REYKJANET stations are equipped with Guralp CMG-3ESPC seismometers and Nanometrics Centaur digitizers and record undistorted ground velocity in the range from 0.03 to 90 Hz with the sampling rate of 250 Hz.

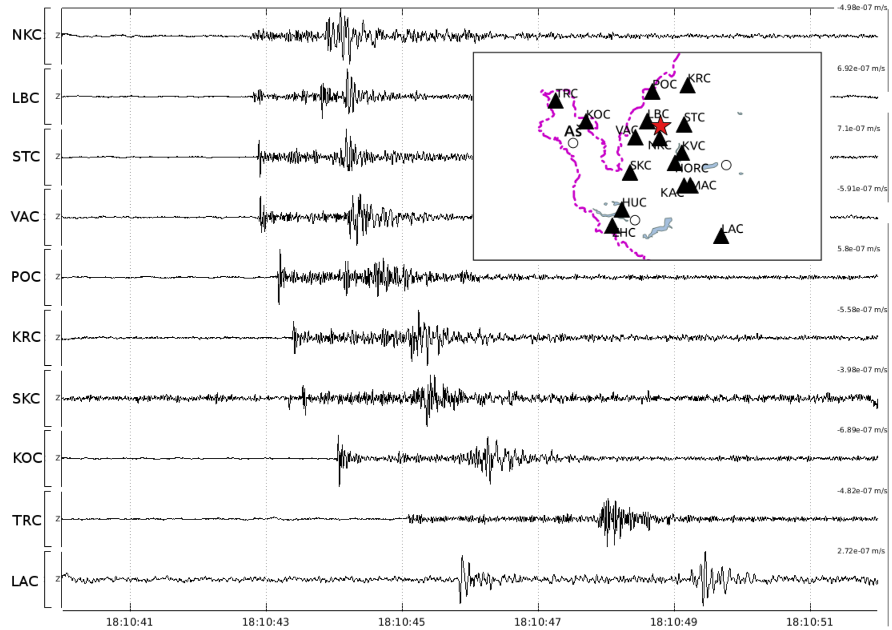

(a) Origin time: December 1, 2018, 18:10:40.916 UTC, depth $d = 9.2\,\mathrm{km}$

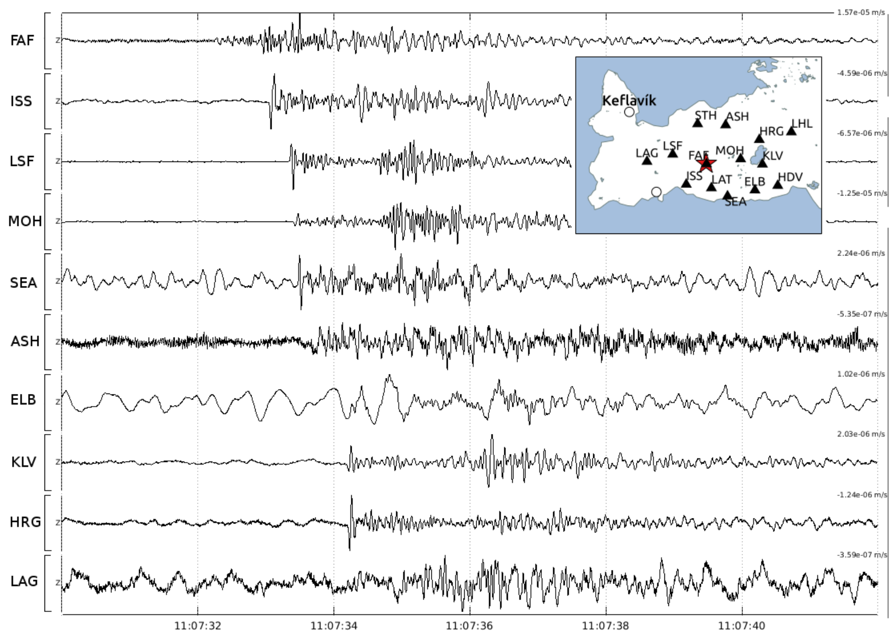

(b) Origin time: July 26, 2017,11:07:31.554 UTC, depth $d = 2.5\,\mathrm{km}$

Figure 1: Waveform examples for (a) WEBNET and (b) REYKJANET events with local magnitude $M_L = 0.5$ (epicenter denotes red asterisks in the insets) located in the center of the seismic networks at depths characteristic of West Bohemia/Vogtland and the Reykjanes Peninsula. Only vertical components of the ground-motion velocity filtered by bandpass of 1–40 Hz at 10 stations with the best signal-to-noise ratio are depicted. All traces are scaled according to the maximum of absolute value of displayed waveform. It is apparent that the noise is generally lower at the WEBNET stations and that the seismograms from the REYKJANET stations are more complex with longer codas which makes their interpretation more demanding.

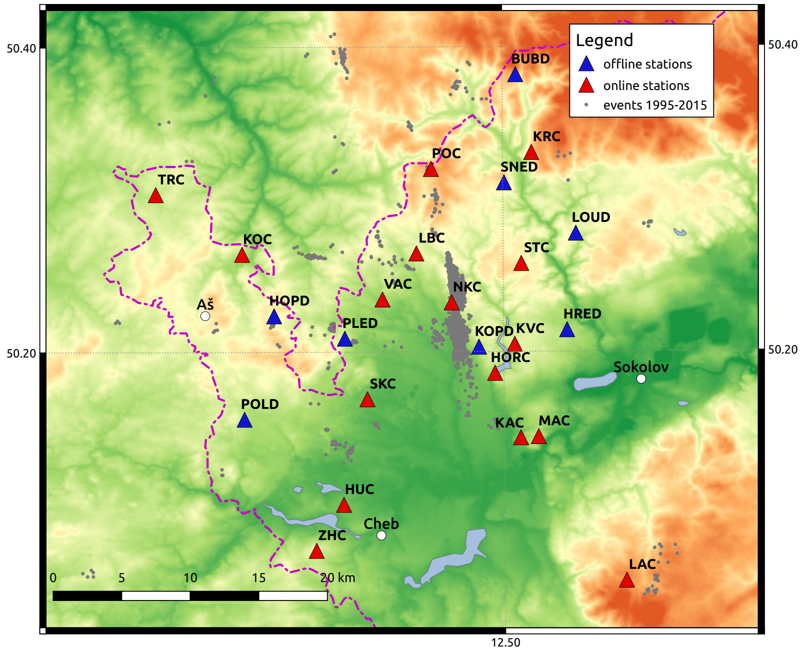

(a)

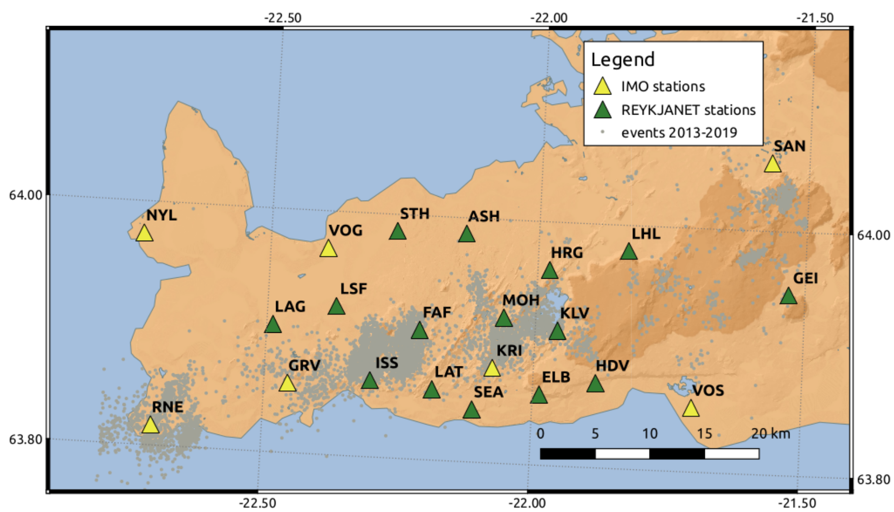

(b)

Figure 2: Maps of WEBNET and REYKJANET seismic networks: (a) WEBNET network before upgrade in 2019. Red triangles denote on-line stations and blue triangles denote off-line stations. The light grey dots represent epicenters of earthquakes in the period 1995-2015, (b) Green triangles are the locations of REYKJANET network stations. Yellow triangles are stations of the regional network SIL operated by Icelandic Meteorological Office (IMO). One can see that REYKJANET network is denser than the SIL network in the area of Reykjanes peninsula. The light grey dots mark the epicenters of earthquakes according to IMO catalog (local magnitude $M_L > 0.5$) in the period 2013-2019.

4 Automatic event detection

4.1 Event detection methods and machine learning in seismology

Seismic events, the useful part of seismic records for the most of seismological research, occur in just a small fraction of total recorded time even in episodic periods of increased seismic activity, for example, earthquake swarms. The target seismic events recorded on seismic stations may differ in few orders of amplitude and they may have fairly different shape and frequency content. Therefore, the classical STA/LTA or other power-based detector detects also various disturbances and with the aim to detect even weak earthquakes it results in a high number of false detections. Well-performing detection algorithm minimizes false detections while preserving all important information, that is, all target seismic events. In our case we want to detect only local events with completeness magnitude as low as possible. Such reduction of data enables effective processing of events either manually or automatically.

Automatic processing of seismic events could be performed in different ways. The first approach accords with the steps of manual processing. Initially, an event must be detected, then the P- and S-phases are picked and the location of the event is computed using those picks (as in Sleeman and van Eck [1999]). In the second approach, a search is made for all possible P- and S-wave phases to combine them to satisfy the events, which are subsequently located (Le Bras et al. [1994], Dietz [2002], Fischer [2003]). During the third approach a search is made through all possible hypocenters and if a concurrence of theoretical data with observed data is detected the event is declared at tested hypocenter without phase onset picking (Withers et al. [1999], Kao and Shan [2004]). We apply the first processing scheme which begins with detecting an event. There are several methods of detection, which can be sorted into the time domain methods, the frequency domain methods, particle motion processing, and pattern matching (Withers et al. [1998]) or using a combination of these approaches.

All groups of detection can be achieved through the Artificial Neural Networks (ANN hereinafter) - machine learning algorithms inspired by the functionality of the human brain. Several neural network concepts have been used for seismic event detection (e.g. Wang and Teng [1995], Tiira [1999], Madureira and Ruano [2009], Mousavi et al. [2018]).

PePin automatic location (Fischer [2003]) which is used routinely to process the WEBNET data in near-real time applies polarization analysis to find candidate onsets of P- and S-wave phases which are then associated together to define events. The algorithm naturally fails to correctly associate phases in case of complex waveforms (e.g. multiple events) which results in omitting some of the events which can be sometimes of not negligible magnitude.

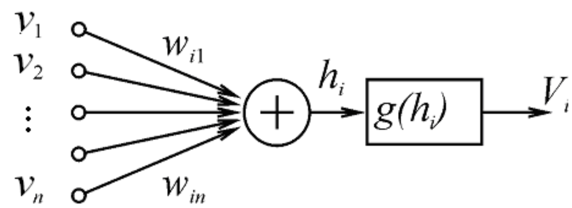

Figure 3: Single i-th neuron with n inputs (from v_1 to v_n), weight coefficients (from w_{i1} to w_{in}), adder with output $h_i = \sum w_{ij}v_j$, activation function $g(.)$ with output $V_i = g(h_i)$.

4.2 SLRNN concept

The advantage of ANN detection methods is the ease of adjusting parameters of detection by training the ANN. Consequently, a detailed description of what are common features for events, or on the other hand, what are the most significant differences between events and disturbances, is not required. The Single Layer Recurrent Neural Network (SLRNN) consists of a set of m artificial neurons. The i-th artificial neuron (Fig. 3) at moment t has an output value

$$V_i = g\left(\sum_{j=1}^{n} w_{ij}v_j\right) \tag{1}$$

where w_{ij} are weight coefficients of the neuron inputs, $v_j(t)$ are input values, $V_i(t)$ is an output value, and $g(.)$ is an activation function. The activation function defines a neuron activation behavior depending on the neuron's weighted input. In this case a widely used hyperbolic tangent is used (the neuron outputs are limited from -1 to 1).

The SLRNN is based on the Real Time Recurrent Network (RTRN, Williams and Zipser [1989]) and the Nonlinear Autoregressive Neural Network (NARX, Narendra and Parthasarathy [1991]). The structure of the Single Layer Recurrent Neural Network is shown in Fig. 4.

Each SLRNN neuron has the following inputs:

$$v_j(t) = \begin{cases} V_K(t-D_c) & j = 1, ..., n_r; K = 1, ..., m; c = 1, ..., d & \text{recurrent inputs} \\ x_i(t) & j = n_r, ..., n-1; i = 1, ..., p & \text{inputs of the SLRNN} \\ 1 & j = n & \text{constant value 1, bias} \end{cases} \tag{2}$$

where m is the number of neurons, n is the number of inputs of each neuron ($n = p + n_r + 1$), p is the number of inputs of the SLRNN, $n_r = m \cdot d$ is the number of recurrent inputs, and d is the number of delay units D_c. As opposed to the RTRN, which has one step delay between output and input, the delay in the SLRNN is variable similar to the NARX. One output of neuron can be connected to many inputs of neurons with different delays. Consequently, there can be more recurrent inputs than neurons. An output of K-th neuron is delayed by D_1 to D_d steps and fed back as a part of the first n_r inputs of the neurons. The use of delays

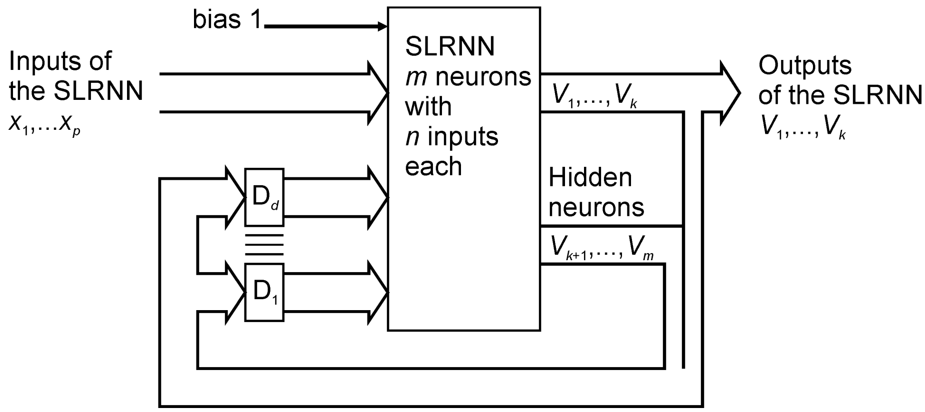

Figure 4: Schema of SLRNN: p inputs of the network $x_1, \ldots, x_p$; k outputs, which are output of neurons $V_1, \ldots, V_k$; and $m-k$ hidden neurons $V_{k+1}, \ldots, V_m$. Output of each neuron is connected to d inputs delayed by the corresponding (D_c) number of cycles, $c = 1, ..., d$. $D_1, \ldots, D_d$ are delay units.

of more time steps allows remembering time relations longer compared to the RTRN design (Wiszniowski et al. [2014]). Thus, the inputs from 1 to n_r are the recurrent ones, the inputs from $n_r + 1$ to $n - 1$ are those of the whole network, and the n-th input (also called bias) is connected to a constant value of 1. As opposed to the NARX design, only a part of neural outputs (k) are outputs of the SLRNN. Other hidden neurons allow building self-adapted time relations not controlled by expected outputs.

The input data of the neural network must be preprocessed before it is used as SLRNN inputs (Fig. 6). Original data is three component seismic records (N, north-south; E, east-west; Z, vertical). First, the signals are filtered by a filter bank. It consists of nine half-octave IIR filters with the narrow frequency bands of 0.6–1 Hz, 1–1.6 Hz, 1.6–2.5 Hz, 2.5–4 Hz, 4–6.3 Hz, 6.3–10 Hz, 10–16 Hz, 16–25 Hz, 25–40 Hz, see Fig. 5. After filtration we compute a total horizontal component $\sqrt{N^2 + E^2}$. Then, we calculate the STA/LTA ratios. The original sampling rate is then decimated to 5 Hz, thus the SLRNN works in 0.2 s time steps. The time step 0.2 s of our SLRNN is a compromise between the acceptable computational load and a good separation of individual waves.

Our SLRNN, designed for detection of small natural earthquakes in WEBNET, consists of 8 neurons and 18 inputs. The feedback connections of the output of each neuron are delayed by 1, 2, 4, and 8 time steps. Thus the neurons have 32 feedback inputs, 18 inputs of the network, and 1 bias input. The 18 inputs come from a filter bank of STA/LTA ratios. The outputs of the first three neurons, which are also outputs of the SLRNN, correspond to: V_1 —detection of event, V_2 —detection of P wave onset, and V_3 —detection of S wave onset. This is achieved by adjusting the weights w_{ij} during the training process. After successful training, the V_1 output is used for event detection, while the rest of the outputs (outputs of the hidden neurons and phase detections) are used only as feedback. The detection outputs V_2 and V_3 cannot be used as pickers because of a long time step of the SLRNN being 0.2 s.

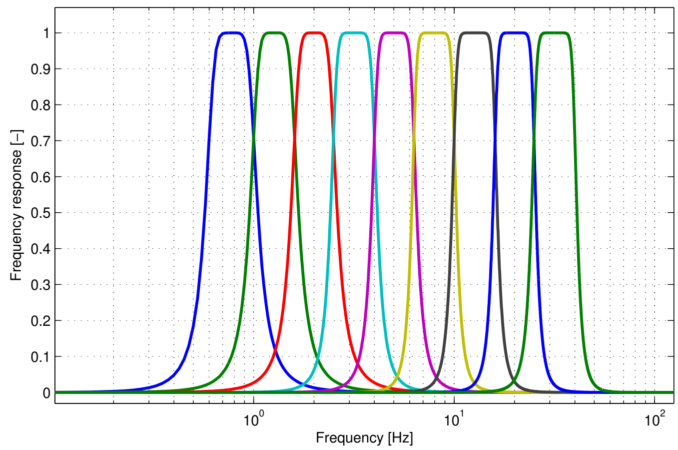

Figure 5: Filter bank frequency response. Each half-octave filter filters out a narrow frequency band from the input signal.

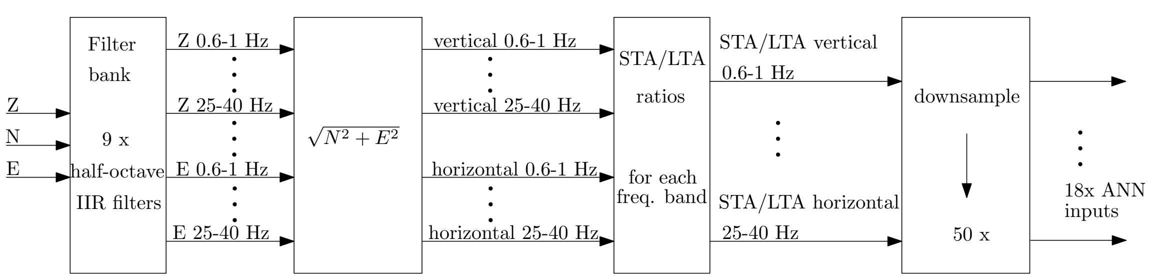

Figure 6: Processing scheme of the SLRNN input data. Three-component raw seismograms are processed into 18 SLRNN inputs.

4.3 The training process

A suitable training of an ANN is of key importance for proper performance of the ANN, so that training of our SLRNN network is one of the most exacting tasks and forms a significant part of my thesis.

We applied a supervised learning algorithm, which means that neuron weights w_{ij} (408 weights in our case) are adjusted in order to get the best possible fit of the real and required outputs of the SLRNN. It is achieved by minimizing the cost function of real and required outputs. Consequently, the required outputs of the network and the cost function E must be defined. The output of a well-trained network ought to fall below a certain threshold during the occurrences of seismic noise and disturbance, whereas it must significantly exceed the threshold during the seismic local event. In our case, the threshold was zero. However, the detection is not required to exceed the threshold at the beginning of the event. It can occur any time during the event. It is not even recommended to exceed the threshold at the beginning until, for example, secondary waves come. Otherwise, some disturbances similar in shape to the P waves might generate detection. Therefore, the required output is negative at the beginning of an event, whereas after the S onset the positive output is strongly enforced. The error between required and real output is weighted in order to ignore or emphasize the error. The cost function E for one waveform in the training set is defined as a sum of output errors in the form:

$$E = \sum_t \sum_{i=1}^{3} \eta_i\,(t)\,[\zeta_i(t) - o_i(t)]^2\,, \tag{3}$$

where ζ_i is the expected output of i-th neuron, η_i is the learning-error weighting coefficient (learning coefficient hereafter) and o_i is the real output of the SLRNN ($i = 1, 2, 3$, corresponding to outputs V_1, V_2 and V_3). Time t is discrete in time steps of the SLRNN which is 0.2 s in our case. Both ζ and η depend on the P and S phases of the seismic event. The learning coefficient defines how sensitive is the learning process of SLRNN to certain periods of the event waveform (Fig. 7). To improve generalization of the detection, we implemented the weight decay regularization method (Hinton [1989]) into SLRNN learning. Then the cost function is

$$E = \gamma \sum_t \sum_{i=1}^{3} \eta_i\,(t)\,[\zeta_i(t) - o_i(t)]^2 + (1-\gamma) \sum_{i=1}^{m} \sum_{j=1}^{n} w_{ij}^2. \tag{4}$$

where the regularization parameter γ controls the extent to which the second penalty term influences the cost function. The minimization is based on a gradient of (4) according to the formula

$$\frac{\partial E}{\partial w_{pq}} = 2\gamma \sum_t \sum_{i=1}^{3} \eta_i\,(t)\,[\zeta_i(t) - o_i(t)]\,\frac{\partial o_i(t)}{\partial w_{pq}} + 2\,(1-\gamma)\,w_{pq}. \tag{5}$$

The Back Propagation Through Time algorithm (Werbos [1990]) was chosen to compute the gradient of cost function. The definition of the expected outputs

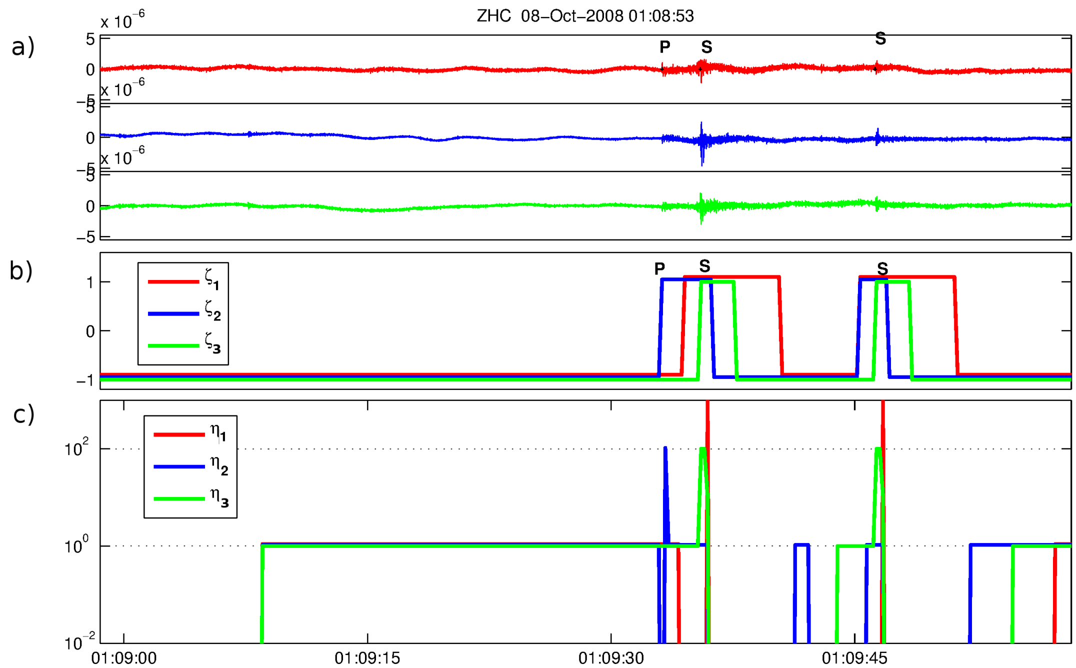

Figure 7: Example of SLRNN learning on the ZHC station from the 8 Oct 2008 event with P- and S-wave onset picks, and a later event with S-wave pick only. a) the seismic signal with marked phases, red - Z component, blue - N component, green - E component, b) expected outputs of the SLRNN, red - event detection, blue - P wave detection, green - S wave detection, c) learning coefficient, red - event detection, blue - P wave detection, green - S wave detection.

$\zeta_1(t), \zeta_2(t), \zeta_3(t)$ (Fig. 7b) and learning coefficients $\eta_1(t), \eta_2(t), \eta_3(t)$ (Fig. 7c) can be found in detail in Doubravová et al. [2016].

The training data was divided randomly into an actual training set (80% of data) and the validation set (20% of data). Each step of the training procedure reduces the cost function of the training set and in addition computes the cost function of the validation set, which is not used for training. As long as the cost function of the training set and cost function of the validation set decrease, training continues. When the cost function of the validation set starts to increase, the training stops. This prevents over-training the network when it would perfectly detect the training events but would not recognize other events well. Because of the strong nonlinearity of the cost function, the training was performed numerous times with different random initial neuron weights w_{ij}. For training the SLRNN we used data from the earthquake swarms of 2008 and 2010. The 2008 data include thousands of local swarm events with manually picked P- and S-wave onsets which are consistent throughout the whole period. We chose randomly about one hundred events for each station with various magnitudes, locations or focal mechanisms. Additionally, a similar number of examples of disturbances and non-local events were needed. For this purpose we chose the 2010 data because it exhibited low local seismicity without

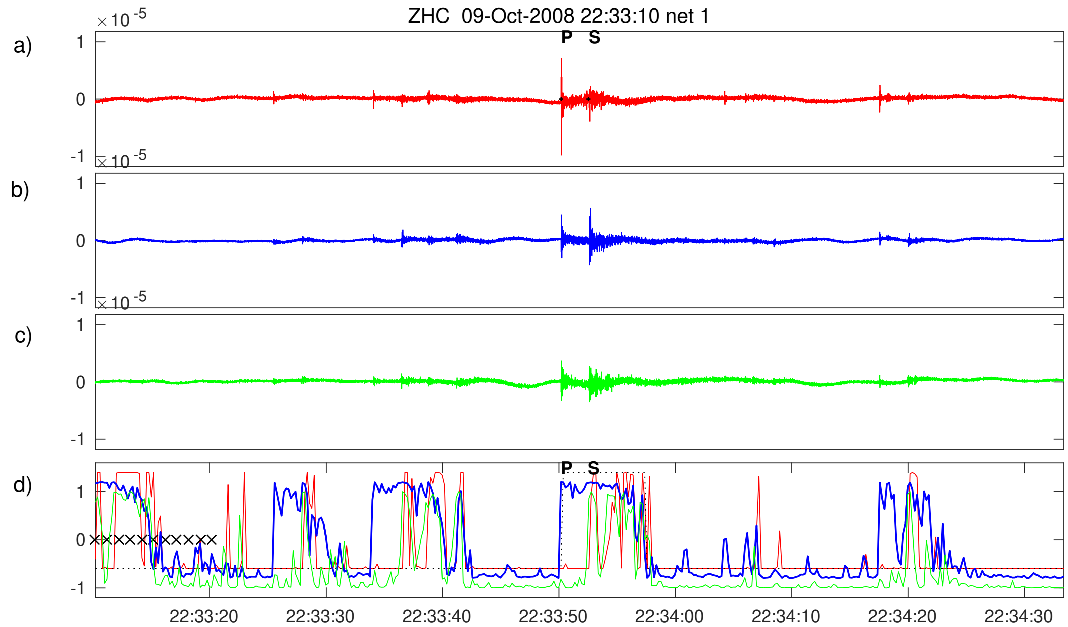

Figure 8: An example of one properly picked event and events not picked (before and after the picked event). Seismogram (the ground velocity in m/s) from station ZHC: (a) Z component with marked phases, (b) N component, (c) E component, (d) detection signals: red – event detection, blue – P wave detection, green – S wave detection.

earthquake swarms. We used manually classified quarry blasts, regional or teleseismic events, disturbances by wind or storms and other unspecified disturbances. Major problems in our training process are lacking picks which may be due to higher noise masking onsets or to unclear P-wave onsets on stations lying near nodal planes of a particular event, rarely due to a failure during the manual processing. When the P- and S-wave picks are missing, the SLRNN network is forced to learn that the signal is a disturbance, causing the training to act in just the opposite way. Additionally, during the evaluation of network performance on the test set many right detections not verified by manual picks are wrongly treated as false detections. To eliminate this problem it was necessary to re-process manually both the training and test sets several times to complete the P- and S-wave onset picks even if their right position was not clear. An example of an unpicked event is shown Fig. 8. At least three events were unpicked. They were detected by the SLRNN.

4.4 Multiple station detection

In order to reduce the number of false detections as well as the number of undetected events due to higher signal-to-noise ratio we search for detection on other stations in the network to confirm or discard the event detection. I designed a simple algorithm that rejects all detections which are not accompanied by enough detections on other stations of the seismic network. The proposed algorithm first scans all detections (detection output above zero) on all stations of the seismic network and checks if there is a detection on a sufficient number of stations in the selected time window (we set it to 5 s with respect the size of the WEBNET and REYKJANET networks). In the next step we combine the detections together to make time intervals for events. As a result we define time segments containing useful information. Thus, multiple overlapping events, especially during a swarm, lead to one time interval containing more events.

The number of stations, which are needed to declare an event, is closely related to the number of false detections. Additionally, too many stations required might cause loss of weaker events. Fig. 9 shows an example of a coincidence of four and six stations and their comparison with the events detections performed manually (by the experienced interpreter). If we compare the detection results of the four- and six-station coincidence with a precise manual ones, it can be seen that the six-station coincidence detects all the manually identified events correctly while four-station coincidence detects also false events or events which are not interpretable. Moreover, four station coincidence detecting more events which merge into a wave train produce longer time window for detections of the events (broader stripes in Fig. 9). Two clearly separated event detections in six-station coincidence may merge into one longer event detection in case of four-station coincidence. For both networks the coincidence of six stations seems to be the best option.

4.5 Application to WEBNET and REYKJANET seismograms

The WEBNET data are first processed by the PePin software (Fischer [2003]) providing automatic locations in near-real time which are sufficient for preliminary interpretations. The events located by PePin are then re-interpreted by manual processing. In order to get good location residuals, the PePin software is set up to use only eight nearest stations around the Nový Kostel focal zone (the central part of the network) which contains more than 90 percent of the total seismic moment released in the whole seismoactive area since 1991 Jakoubková et al. [2018]). This unfortunately may result in omitting events outside the main focal zone. During November–December 2018 we compared in detail all event detections by the SLRNN with precise manual readings and with the PePin results. In this period the local seismicity was extremely low with maximum magnitude $M_{Lmax} = 1.3$. We took into account only events with magnitude above $M_L = -0.5$, which resulted in 183 events. The results of our analysis are displayed in Fig. 10a. There are 106 events of $M_L > -0.5$ successfully detected by both SLRNN and PePin (red circles in Fig. 10a), 73 events were successfully detected by the SLRNN only (they are missing in the PePin catalog, yellow circles in Fig. 10a), and four events missing in the SLRNN list were successfully located by PePin (green circles in Fig. 10a).

It is worth mentioning that significant part of the undetected events by the PePin algorithm are located outside the main focal zone of Nový Kostel. The six-station coincidence, which we found to be an optimum for the West Bohemia/Vogtland

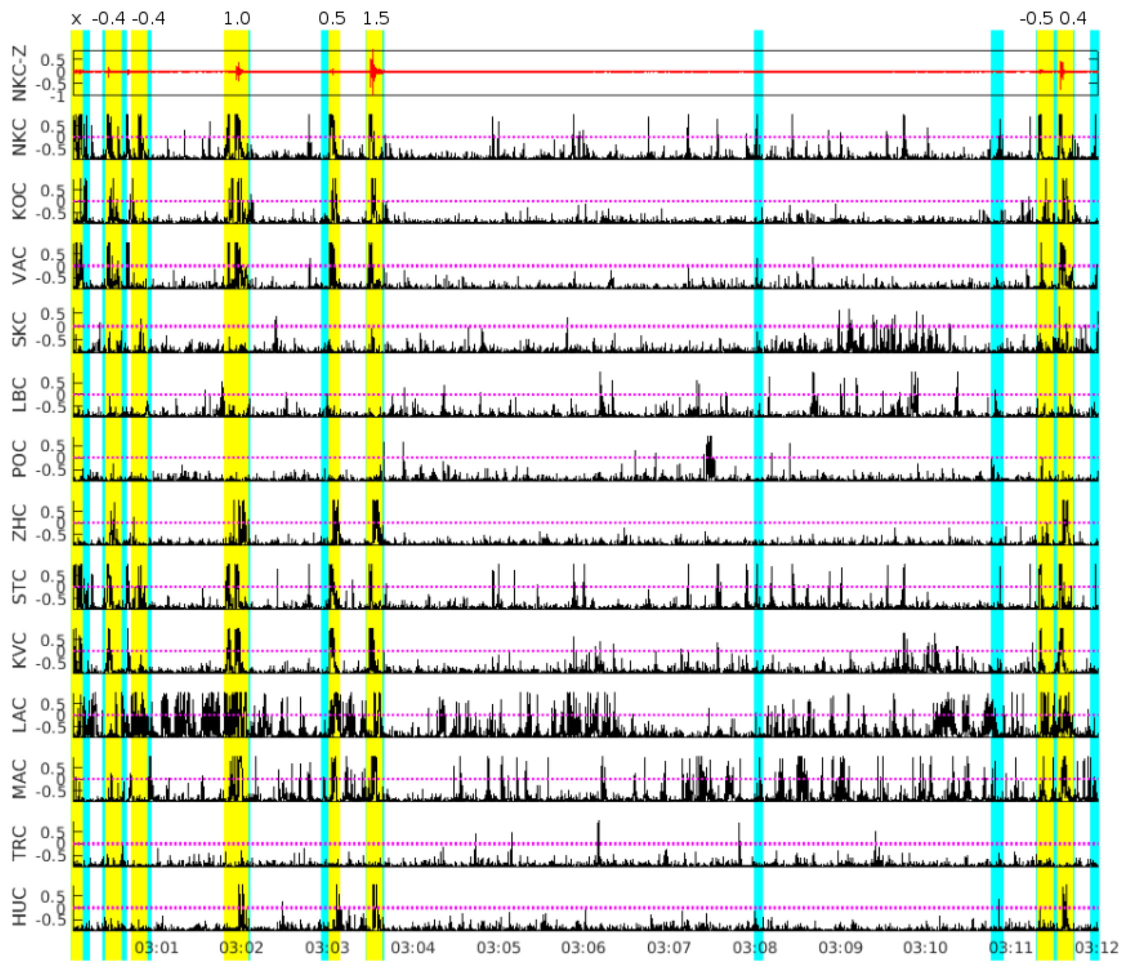

Figure 9: Example of the detection coincidence for four (cyan) and six (yellow) WEBNET stations. In case of concurrent event detection by four and six station coincidence the cyan stripes are overlaid by the yellow ones. Red trace above is the vertical component of seismogram from NKC station from 2018 August 24 3:00–3:12 UTC. All events in yellow were also detected manually, magnitudes M_L (from -0.5 to 1.5) are given above the yellow stripes. The first detected event in the seismogram is a multiple event consisting of several weak overlapping events, therefore the magnitude is not assigned (x sign is printed instead). Note the end of the record where two yellow events merge into one longer cyan event.

earthquake-swarm region, results in omitting four events which were located both manually and by PePin; all four undetected events have magnitude $M_{Lmax} \approx -0.5$. If we use four-station coincidence then all manually located events are successfully detected by the SLRNN but the number of event detections increase significantly.

A potential ANN trained on the South-West Iceland data from REYKJANET poses quite a big problem because of the absence of complete catalogs/bulletins from the REYKJANET network which would be necessary to train the ANN. It is because of the REYKJANET recordings that have not been fully processed in detail like the WEBNET ones. To create relevant bulletins from the REYKJANET stations by manual processing of continuous recording would be extremely time-consuming, requiring an experienced specialist. Consequently, we mostly use the catalogs of a regional Icelandic network SIL provided by Icelandic Meteorological Office (IMO) for the REYKJANET-data analysis. Therefore, an application of the SLRNN network trained for the West Bohemia/Vogtland data (WEBNET) to data from South-West Iceland (REYKJANET) has been a challenging task. I used one of the best-performing SLRNNs as tested for WEBNET and applied it to the REYKJANET data. Since the deployment of the REYKJANET network in 2013, the seismicity on the Reykjanes Peninsula has typically been on a micro-earthquake level (magnitudes $M_L < 3$) except two earthquake swarms in October 2013 (which occurred on the tip of the peninsula out of the REYKJANET network immediately after putting the stations into operation) with $M_{Lmax} = 4.8$ and in July 2017 with $M_{Lmax} = 3.9$, and few weaker swarm-like episodes with magnitudes up to $M_{Lmax} = 3.5$. We analyzed in detail the detection results for

(i) four weak swarm-like activities from the period 2014–2015,

(ii) an intensive $M_{Lmax} = 3.9$ swarm of July 2017 and

(iii) scattered background seismicity on the Reykjanes Peninsula in June 2017

The SIL catalog is the primary reference for evaluation of the SLRNN-detection results for both (i) and (ii). Besides, we used a catalog of the event detections produced by PePin algorithm and Antelope software package (by Boulder Real Time Technologies, Ltd.) that were applied to the REYKJANET data (i), and a detailed bulletin of the 2017 swarm containing manual onset picks from all the REYKJANET stations.

(i) First, we compared the total number of detected events by the SIL processing at IMO, PePin algorithm, Antelope software and SLRNN in the individual weak activities (see Fig. 11). The number of events detected by SIL, PePin and Antelope is comparable for all the activities, while the number of detected events by the SLRNN is about five times higher. We manually checked one of the activities with a reasonable number of events—the mini-swarm of the 2015 March 31 (Fig. 12). Inspecting the events manually, we found out none of the 'catalogs' (SIL, Antelope and PePin) to have been a complete subset of another one; each catalog contained some unique events which were missing in the other two catalogs. By combining the SIL, PePin and Antelope catalogs we obtained 51 real events with minimum magnitudes $M_L \approx 0$. Our SLRNN detected all of them and in addition to that about three times more weak events. But many of the small detected events are unsuitable for further processing because locating of such events would be unreliable

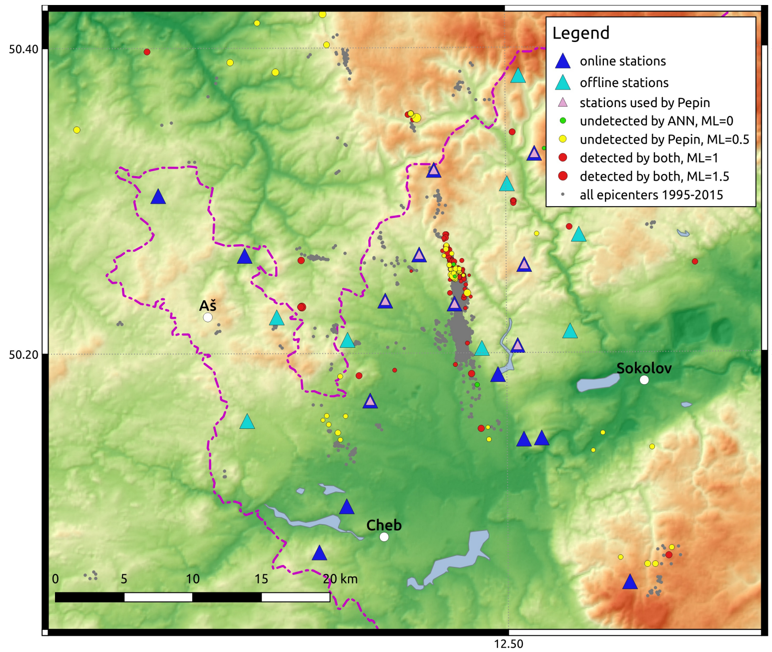

(a)

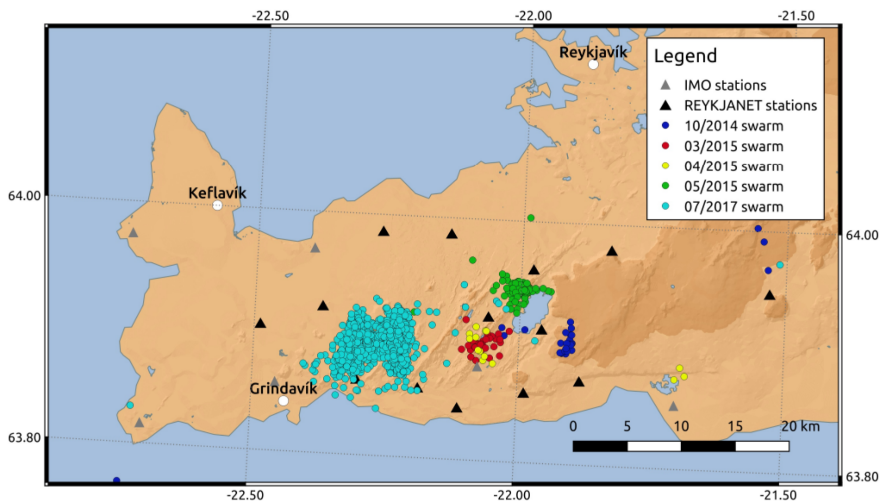

(b)

Figure 10: Results of SLRNN application to WEBNET and REYKJANET data. (a) Detection of local events during November and December 2018 in West Bohemia/Vogtland. Red circles – events located manually and by PePin and also detected by SLRNN, yellow circles – events located manually and detected by SLRNN (not located by PePin), green circles – events located manually and by PePin (not detected by SLRNN). (b) Analyzed seismic activities on the Reykjanes Peninsula. Blue circles – 2014 October 30–31 ($M_{Lmax} = 2.8$), red circles – 2015 March 31 ($M_{Lmax} = 2.2$), yellow circles – 2015 April 28–30 ($M_{Lmax} = 1.6$), green circles – 2015 May 29–30 ($M_{Lmax} = 3.5$), cyan circles – 2017 July 26–28 ($M_{Lmax} = 3.9$).

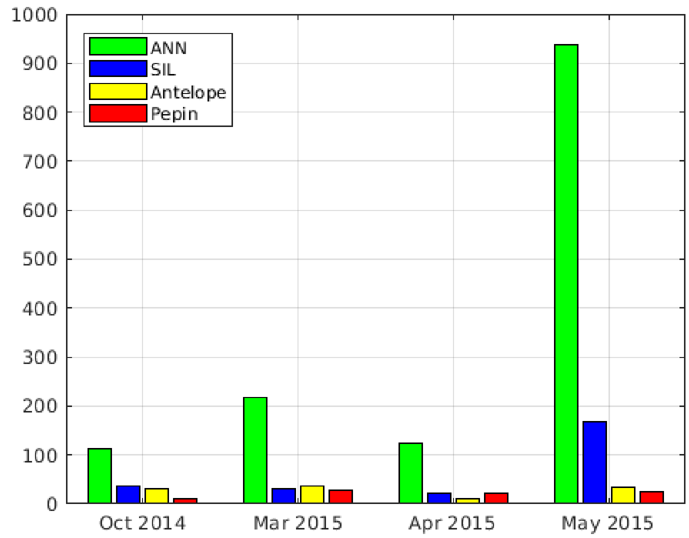

Figure 11: Number of detected events in analyzed micro-swarms on the Reykjanes Peninsula.

due to unclear P- and S-wave onsets.

(ii) A prominent earthquake swarm in July–August 2017 $M_{Lmax} = 3.9$ was fairly rapid. Most of the seismic moment released during 2 days from July 26 to 28 (Jakoubková [2018]), more than 1500 $M_L > 0$ events have been listed in the SIL catalog for these days. We concentrated on 1 hr of the swarm activity on July 26, from 11:00 to 12:00 UTC, that included the second strongest earthquake of the swarm ($M_L = 3.7$). This segment contains both calm and turbulent phase of the swarm. We performed detailed manual processing of the continuous seismograms with the assistance of an experienced expert who found 441 events in total out of which 281 were reliably located with magnitude above $M_L > 0$. Then we compared the manually obtained events with detections provided by the SLRNN and with the list of events in SIL catalog (Fig. 13). All of the manually picked events were correctly detected by the SLRNN and only one false SLRNN detection was found.

(iii) In order to prove the SLRNN ability to detect various local events on the whole Reykjanes Peninsula we selected a time segment containing scattered background non-swarm seismicity only. We selected one week, 2017 June 6–12, where the seismic events included in the SIL catalog were scattered in the whole area covered by the REYKJANET network. The SLRNN detected 183 events, 34 events of which had been listed in the SIL catalog and no event present in SIL catalog was missed. By manual processing of the waveforms we were able to confirm reliably 37 new events which we located and for which we estimated M_L ranging from -0.5 to 1.3 (30 above $M_L = 0$). Remaining 112 events were mostly unfit for location due to insufficient number of clear P- and S-wave onset picks or they were real events hidden in ambient noise, and probably some of them were also false alarms.

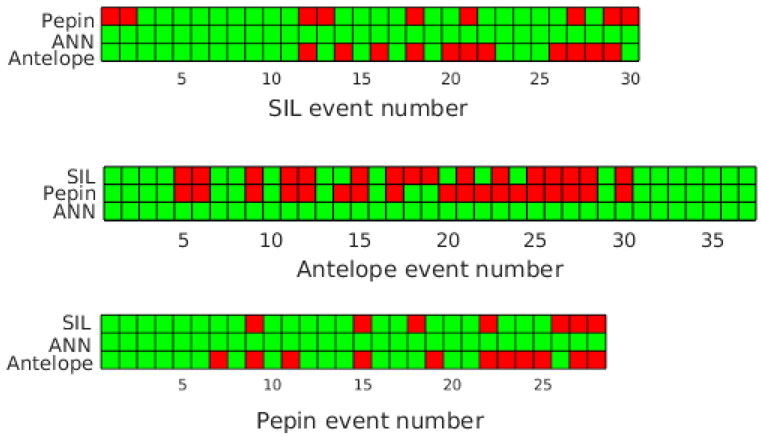

Figure 12: Detailed examination of the SLRNN detection results and the SIL, Antelope and PePin catalogs for mini-swarm of 2015 on the Reykjanes Peninsula. The diagrams represent the individual catalogs; from top to bottom: SIL, Antelope and PePin. Each column in the individual diagrams denotes a particular event in the respective catalog (thus the number of columns in each diagram equals to the number of events in the catalog). The events in the SIL and PePin diagrams are ordered according to magnitudes M_L given in the SIL and PePin catalogs from the strongest (on the left) to the weakest one (on the right); the events in the Antelope diagram are sorted according to the origin time. The rows in the diagrams denote events which are included (green cells)/missing (red cells) in the remaining three catalogs (indicated on the right). Note that the each catalog (SIL, Antelope and PePin) contains some events detected only by ANN and missed in the other two catalogs.

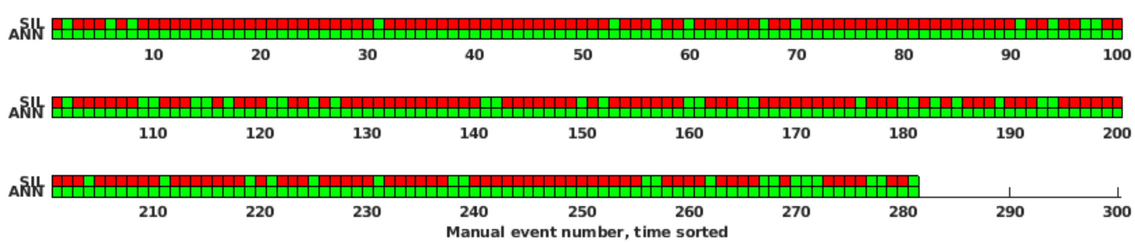

Figure 13: Comparison of the SLRNN detection results with the SIL and manual REYKJANET catalog for 1 hr period of a larger 2017 swarm on the Reykjanes Peninsula. High rate seismicity in the time window of 2017 July 26, 11:00 to 12:00 UTC, is examined. The diagram represents a comparison of the SLRNN results and SIL catalog with the REYKJANET catalog (281 M_L >0 events) created manually by an experienced interpreter. The events are sorted according to the origin time.

5 Seismon_WB

Seismon_WB is a software which enables the interpreters to work with seismic data comfortably using graphical user interface (GUI). The experts in seismic-data processing and analyses do not need programming skills or heavy training to work with this user-friendly intuitive software. On the other hand anyone can develop new functions directly using MATLAB.

Seismon_WB is a modification of software Seismon created by Stefan Mertl in MATLAB (Mertl and Hausmann [2009]), in 2011 the original Seismon started to be rewritten in Python under a new name pSysmon (`http://www.mertl-research.at/projects/psysmon/`). The original program Seismon was designed as an universal tool for seismic experiments. For that purpose it consists of various tools and modules that can be adapted and developed by the users. The main advantage of that software is the close connection with the MySQL database. The database enables to store the results, network configuration, information about instruments used on particular stations at specific time and a list of available waveform files and the description of their contents. Well organized database is very important property of a software used for routine processing. But original Seismon did not meet all the requirements for routine processing of continual recordings from the WEBNET stations. It was therefore necessary to change many tools, often the whole behavior of the software and develop number of new modules to satisfy specific needs for the WEBNET data processing. This way I developed a new branch of Seismon differing significantly from the former one, which we started to call Seismon_WB (Seismon for the WeBnet data processing).

Seismon_WB replaced an obsolete program Seisbase (Fischer and Hampl [1997]) in 2013 and became the main processing tool for WEBNET data. Before introducing the Seismon_WB in daily routines for the WEBNET data we took care to ensure a compatibility with Seisbase and thus to preserve the consistency of the results over the years. The behavior of Seismon_WB has been adapted to work similar to Seisbase in order to be comfortable for the interpreters used to the former program. Seisbase targeted to WEBNET data from the beginning was equipped with many useful functions making a primary seismogram processing and data analyses more effective. However, Seisbase was unable to handle miniSEED file format, continuous records in general and it gradually became complicated to run this DOS-based software on new computers. I consulted the most common steps in routine work with the experienced interpreters and modified the program to be as helpful as possible for the users. That resulted in fairly comfortable software which on contrary lost some of its original universality. Seismon_WB has been used in continuous regime from September 2014.

The Fig. 14 shows the data flow around Seismon_WB. The program itself serves as an interface for the user that enables to access and process various data sets and to call external programs. The primary storage is MySQL database mainly accessed by Seismon_WB but it could be also fed by external programs. Most of the external programs used for data interpretation (location, moment tensor inversion etc.) are called by Seismon_WB and their results are saved to the database by Seismon_WB

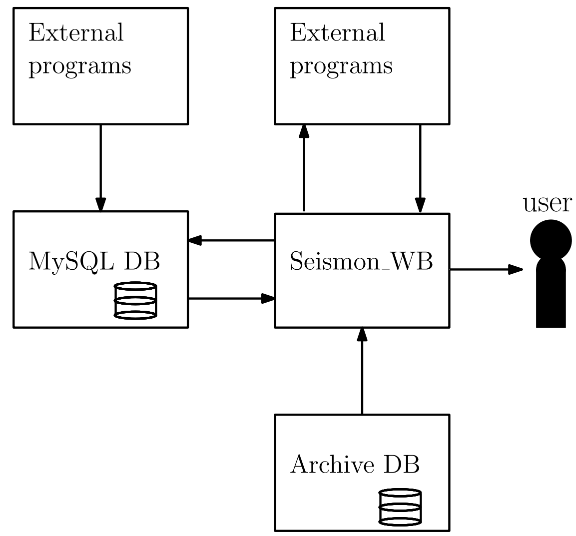

Figure 14: Seismon interaction scheme. The user interacts with Seismon_WB software to access the database and external programs. The archive data exported from Paradox database can be converted to MySQL database tables with Seismon_WB structure using specific packages of Seismon_WB itself.

itself. The Archive DB block represents the export from Paradox database (formerly used by Seisbase) which can be converted to MySQL Seismon structure using specific Seismon_WB package of functions. This is one of the features that enabled the compatibility between Seismon_WB and Seisbase.

Seismon is designed as a modular software in order to be highly flexible and effective. The task that needs to be performed is achieved by a sequence of modules, which are functional units performing particular operation. An ordered set of modules is called a collection; typically each user defines few such collections for his/her own needs. The basic objects and philosophy of original Seismon were mostly preserved, although I developed many new modules and modified the most of the existing ones.

Seismon is equipped with modules for viewing, modifying and exporting the database, working with events, data files and waveforms. Some modules are standalone, others need to be preceded or succeeded by another module, some modules are editable and by setting the parameters we define the input arguments of the module function. The parameters are set by using dialog windows.

In fact the automatic processing as a part of Seismon_WB itself or as an external program can be used at any stage of the processing and the visual inspection of automatic procedures can be comfortably supervised using Seismon_WB.

The program is written in MATLAB which offers advantages of well documented toolboxes and functions easy to use. Due to limits of free MATLAB software spreading I also created standalone version of Seismon_WB, that can be run without MATLAB license.

Seismon_WB can be generally used on Windows, Linux and MAC platforms, however only Windows and Linux versions have been tested.

The development of the Seismon_WB software is still continuing adapting to new requirements of the users for new or improved functionality, the compatibility with up-to-date version of MATLAB is consistently maintained.

6 Conclusion

Dense local seismic networks WEBNET and REYKJANET contribute to detailed studies of the seismic swarms dynamics, earthquake source and local structure of the Earth's crust. Without the automatic and semi-automatic processing of the seismic networks WEBNET and REYKJANET it would be impracticable to process the measured data in a full extent. My thesis consists of two parts: (i) Seismon_WB - a software for interactive data processing that enables also to control automatic and semi-automatic processing; and (ii) SLRNN detector of seismic events which is the fundamental step in automatic seismic data processing. The design, training, detailed testing and implementation of the SLRNN form a core part of this doctoral thesis and is described in detail in two attached papers.

(i) First, I needed to concern the comfortable way to manually process the seismic data. I contributed extensively to a development of new software used by the WEBNET working group by modifying, extending and debugging an existing Seismon project. As a result Seismon_WB is an exclusive processing tool for all the routines applied to WEBNET (and REYKJANET) data since 2013. Not only classical manual processing is achieved by Seismon_WB but also an evaluation and check of automatic procedures applied. Nevertheless, the tuning and development of the software still continues. Although the software development is strictly practical result with very low direct scientific impact, it is an essential prerequisite for high quality processing of seismic data provided by the WEBNET group.

(ii) Next, the detection algorithm has been developed, tested and introduced into practice. We designed a new artificial neural network concept and successfully applied it not only to WEBNET data used for training the neural network but also to data from REYKJANET network. The trained SLRNN is nowadays routinely used to detect events in recordings of local seismic networks WEBNET and REYKJANET.

The main results and lessons learned from the SLRNN may be summed up as follows:

- The SLRNN architecture is suitable for seismic event detection and eight neurons proved to be sufficient. The higher number of neurons does not improve the performance significantly as the training demands rise considerably. The detection performance is enhanced by coincidence in the network.

- The training data must be prepared with special care, missing P- and S-wave onset picks (especially if both are missing) complicate the proper training giving bad examples during the training. Even rough picks of noisy events helped the training significantly.

- The training using gradient-based methods requires many trials to repeat to find the optimum result. To evaluate the real detector performance, the sensitivity, specificity and precision quantities must be used. To check the detection results properly a lot of manual work is needed, because many of the SLRNN detections are low-magnitude events which are often missing in available catalogs.

- It is impossible to achieve good results with low completeness magnitude using one station detection. For fine result a coincidence in the network of seismic stations must be used. Six stations coincidence is a reasonable choice for both WEBNET and REYKJANET local seismic networks.

- Well-trained network can be successfully used for different region and a partly different types of waveforms. This is the generalization property of a neural network and the successful applicability of the detector trained on WEBNET data to REYKJANET data is an exemplary utilization of that.

In the near future there is a potential to use our neural network to pre-process data of the NEFOBS (Near Fault Observatory) deployed in the West Bohemia/Vogtland region consisting of four broad-band seismometers placed in shallow boreholes ($\approx$ 400 m deep) drilled within ICDP project *Drilling the Eger Rift* (more on `https://www.icdp-online.org/projects/world/europe/eger/` or Dahm et al. [2013]) supplemented with 3-D seismic arrays. The expected significantly larger amount of high-frequency micro-events (with local magnitudes as low as $M_L \approx -2$) might be successfully detected by our SLRNN.

The event detection is a starting point in the data processing chain for both automatic and manual processing. Its quality affects the whole processing results. I believe, I proved that the presented method provides high quality detections suitable for effective post-processing and thus high-quality investigation of the seismicity of the West Bohemia/Vogtland as well as South-West Iceland and potentially any other seismically active region.

Bibliography

H. Čermáková and J. Horálek. The 2011 West Bohemia (Central Europe) earthquake swarm compared with the previous swarms of 2000 and 2008. *Journal of Seismology*, pages 1–15, 2015. ISSN 1383-4649. doi: 10.1007/s10950-015-9502-3. URL `http://dx.doi.org/10.1007/s10950-015-9502-3`.

T. Dahm, P. Hrubcová, T. Fischer, J. Horálek, M. Korn, S. Buske, and D. Wagner. Eger rift ICDP: an observatory for study of non-volcanic, mid-crustal earthquake swarms and accompanying phenomena. *Scientific Drilling*, 16:93–99, 2013. doi: 10.5194/sd-16-93-2013. URL `https://www.sci-dril.net/16/93/2013/`.

L. Dietz. Notes on configuring BINDER_EW: Earthworm's phase associator, 2002. URL `http://www.isti2.com/ew/ovr/binder{_}setup.html`.

J. Doubravová, J. Wiszniowski, and J. Horálek. Single layer recurrent neural network for detection of swarm-like earthquakes in W-Bohemia/Vogtland - the method. *Computers & Geosciences*, 93:138 – 149, 2016. ISSN 0098-3004. doi: https://doi.org/10.1016/j.cageo.2016.05.011. URL http://www.sciencedirect.com/science/article/pii/S0098300416301327.

T. Fischer. Automatic location of swarm earthquakes from local network data. *Studia Geophysica et Geodaetica*, 47(1):83–98, 2003. ISSN 0039-3169. doi: 10.1023/A:1022251605990. URL http://dx.doi.org/10.1023/A%3A1022251605990.

T. Fischer and F. Hampl. SEISBASE - Principles of a Program and Database for Routine Analysis of Data from Local Seismic Networks, Version 4.7. *Acta Montana*, Ser. A(11):15–34, 1997.

T. Fischer, J. Horálek, J. Michálek, and A. Boušková. The 2008 West Bohemia earthquake swarm in the light of the WEBNET network. *Journal of Seismology*, 14(4):665–682, 2010. ISSN 1383-4649. doi: 10.1007/s10950-010-9189-4. URL http://dx.doi.org/10.1007/s10950-010-9189-4.

T. Fischer, J. Horálek, P. Hrubcová, V. Vavryčuk, K. Bräuer, and H. Kämpf. Intra-continental earthquake swarms in West-Bohemia and Vogtland: A review. *Tectonophysics*, 611:1 – 27, 2014. ISSN 0040-1951. doi: https://doi.org/10.1016/j.tecto.2013.11.001. URL http://www.sciencedirect.com/science/article/pii/S0040195113006458.

T. Fischer, C. Matyska, and J. Heinicke. Earthquake-enhanced permeability - evidence from carbon dioxide release following the M_L 3.5 earthquake in West Bohemia. *Earth and Planetary Science Letters*, 460:60–67, 2017.

H. Geirsson, T. Árnadóttir, S. Hreinsdóttir, J. Decriem, P.C. LaFemina, S. Jónsson, R.A. Bennett, S. Metzger, A. Holland, E. Sturkell, T. Villemin, C. Völksen, F. Sigmundsson, P. Einarsson, M.J. Roberts, and H. Sveinbjörnsson. Overview of results from continuous GPS observations in Iceland from 1995 to 2010. *Jökul*, 60: 3–22, 2010.

G. E. Hinton. Connectionist learning procedures. *Artificial Intelligence*, 40:185 – 234, 1989. doi: http://dx.doi.org/10.1016/0004-3702(89)90049-0. URL http://www.sciencedirect.com/science/article/pii/0004370289900490.

J. Horálek. Reykjanet, 2013. URL http://www.fdsn.org/networks/detail/7E_2013/.

J. Horálek and T. Fischer. Role of crustal fluids in triggering the West Bohemia/Vogtland earthquake swarms: Just what we know (a review). *Studia Geophysica et Geodaetica*, 52(4):455, Feb 2008. ISSN 1573-1626. doi: 10.1007/s11200-008-0032-0. URL https://doi.org/10.1007/s11200-008-0032-0.

J. Horálek and T. Fischer. Intraplate earthquake swarms in West Bohemia/Vogtland (Central Europe). *Jokull*, 60:67–88, 2010.

J. Horálek, T. Fischer, A. Boušková, and P. Jedlička. The Western Bohemia/Vogtland region in the light of the WEBNET network. *Studia Geophysica Et Geodaetica*, 44(2):107–125, 2000.

A S C R Institute of Geophysics. West Bohemia local seismic network, 1991. URL `http://www.fdsn.org/networks/detail/WB/`.

H. Jakoubková. *Earthquake swarms in diverse tectonic environments*. PhD thesis, Charles University in Prague, 2018.

H. Jakoubková, J. Horálek, and T. Fischer. 2014 mainshock-aftershock activity versus earthquake swarms in West Bohemia, Czech Republic. *Pure and Applied Geophysics*, 175(1):109–131, Jan 2018. ISSN 1420-9136. doi: 10.1007/s00024-017-1679-7. URL `https://doi.org/10.1007/s00024-017-1679-7`.

H. Kao and S. Shan. The source-scanning algorithm: mapping the distribution of seismic sources in time and space. *Geophysical Journal International*, 157 (2):589–594, 2004. doi: 10.1111/j.1365-246X.2004.02276.x. URL `http://gji.oxfordjournals.org/content/157/2/589.abstract`.

R. Le Bras, H. Swanger, T. Sereno, G. Beall, and R. Jenkins. Global association. design document and user's manual. Technical report, DTIC Document, 1994.

G. Madureira and A. E. Ruano. A neural network seismic detector. *Acta Technica Jaurinensis*, 2(2):159–170, 2009.

S. Mertl and H. Hausmann. Seismon-a flexible seismic processing software. In *EGU General Assembly Conference Abstracts*, volume 11, page 4266, 2009.

S. M. Mousavi, W. Zhu, Y. Sheng, and G. C. Beroza. CRED: A deep residual network of convolutional and recurrent units for earthquake signal detection, 2018.

K.S. Narendra and K. Parthasarathy. Gradient methods for the optimization of dynamical systems containing neural networks. *Neural Networks, IEEE Transactions on*, 2(2):252–262, Mar 1991. ISSN 1045-9227. doi: 10.1109/72.80336.

K. Sæmundsson and P. Einarsson. Notes on the tectonics of Reykjanes. report no. ísor-2013/003, 2014.

R. Sleeman and T. van Eck. Robust automatic P-phase picking: an on-line implementation in the analysis of broadband seismogram recordings. *Physics of the Earth and Planetary Interiors*, 113(1–4):265–275, 1999. ISSN 0031-9201. doi: http://dx.doi.org/10.1016/S0031-9201(99)00007-2. URL `http://www.sciencedirect.com/science/article/pii/S0031920199000072`.

T. Tiira. Detecting teleseismic events using artificial neural networks. *Computers I& Geosciences*, 25(8):929 – 938, 1999. ISSN 0098-3004. doi: http://dx.doi.org/10.1016/S0098-3004(99)00056-4. URL `http://www.sciencedirect.com/science/article/pii/S0098300499000564`.

J. Wang and T. Teng. Artificial neural network-based seismic detector. *Bulletin of the Seismological Society of America*, 85(1):308–319, 1995. URL `http://www.bssaonline.org/content/85/1/308.abstract`.

P. J. Werbos. Backpropagation through time: what it does and how to do it. *Proceedings of the IEEE*, 78(10):1550–1560, Oct 1990. ISSN 0018-9219. doi: 10.1109/5.58337.

R. J. Williams and D. Zipser. A learning algorithm for continually running fully recurrent neural networks. *Neural Comput.*, 1(2):270–280, June 1989. ISSN 0899-7667. doi: 10.1162/neco.1989.1.2.270. URL `http://dx.doi.org/10.1162/neco.1989.1.2.270`.

J. Wiszniowski, B.M. Plesiewicz, and J. Trojanowski. Application of Real Time Recurrent Neural Network for Detection of Small Natural Earthquakes in Poland. *Acta Geophys.*, 62(3):469–485, 2014.

M. Withers, R. Aster, C. Young, J. Beiriger, M. Harris, S. Moore, and J. Trujillo. A comparison of select trigger algorithms for automated global seismic phase and event detection. *Bulletin of the Seismological Society of America*, 88(1):95–106, 1998. URL `http://www.bssaonline.org/content/88/1/95.abstract`.

M. Withers, R. Aster, and C. Young. An automated local and regional seismic event detection and location system using waveform correlation. *Bulletin of the Seismological Society of America*, 89(3):657–669, 1999. URL `http://www.bssaonline.org/content/89/3/657.abstract`.

List of publications

Doubravová et al., 2016: J. Doubravová, J. Wiszniowski, and J. Horálek. Single layer recurrent neural network for detection of swarm-like earthquakes in W-Bohemia/Vogtland - the method. *Computers & Geosciences*, 93:138 – 149, 2016. ISSN 0098-3004. doi: https://doi.org/10.1016/j.cageo.2016.05.011. URL `https://www.sciencedirect.com/science/article/pii/S0098300416301327`

Doubravová and Horálek, 2019: J. Doubravová and J. Horálek. Single Layer Recurrent Neural Network for detection of local swarm-like earthquakes—the application. *Geophysical Journal International*, 219(1):672–689, 07 2019. ISSN 0956-540X. doi: 10.1093/gji/ggz321. URL `https://doi.org/10.1093/gji/ggz321`